

# Assessment of mycoviral diversity in Pakistani fungal isolates revealed infection by 11 novel viruses of a single strain of *Fusarium mangiferae* isolate SP1

Haris Ahmed Khan<sup>1,2†</sup>, Wajeeha Shamsi<sup>1†,‡</sup>, Atif Jamal<sup>3</sup>, Memoona Javaied<sup>1</sup>, Mashal Sadiq<sup>1</sup>, Tehsin Fatma<sup>1</sup>, Aqeel Ahmed<sup>1</sup>, Maleeha Arshad<sup>1</sup>, Mubashra Waseem<sup>1</sup>, Samra Babar<sup>1</sup>, Midhat Mustafa Dogar<sup>1</sup>, Nasar Virk<sup>1§</sup>, Hussnain Ahmed Janjua<sup>1</sup>, Hideki Kondo<sup>2</sup>, Nobuhiro Suzuki<sup>2</sup> and Muhammad Faraz Bhatti<sup>1,\*</sup>

## Abstract

An extensive screening survey was conducted on Pakistani filamentous fungal isolates for the identification of viral infections. A total of 396 fungal samples were screened, of which 36 isolates were found double-stranded (ds) RNA positive with an overall frequency of 9% when analysed by a classical dsRNA isolation method. One of 36 dsRNA-positive strains, strain SP1 of a plant pathogenic fungus *Fusarium mangiferae*, was subjected to virome analysis. Next-generation sequencing and subsequent completion of the entire genome sequencing by a classical Sanger sequencing method showed the SP1 strain to be co-infected by 11 distinct viruses, at least seven of which should be described as new taxa at the species level according to the ICTV (International Committee on Taxonomy of Viruses) species demarcation criteria. The newly identified *F. mangiferae* viruses (FmVs) include two partitivirids, one betapartitivirus (FmPV1) and one gammapartitivirus (FmPV2); six mitovirids, three unamitovirus (FmMV2, FmMV4, FmMV6), one duamitovirus (FmMV5), and two unclassified mitovirids (FmMV1, FmMV3); and three botourmiavirids, two magoulivirus (FmBOV1, FmBOV3) and one scleroulivirus (FmBOV2). The number of coinfecting viruses is among the largest ones of fungal coinfections. Their molecular features are thoroughly described here. This represents the first large virus survey in the Indian sub-continent.

## INTRODUCTION

Mycovirus (fungal virus) hunting has been greatly expedited by the recent advances in Next-generation sequencing (NGS) [1–4]. Extensive screening of many phytopathogenic, entomopathogenic, and human-pathogenic fungi and oomycetes has been performed in the past decades [5–11]. Different incident rates (from a small number of percentages to more than 90%) have been reported in plant-related fungi [12]. Mycoviruses have also been reported in various types of fungi,

including cultivated and wild mushrooms, and saprophytic litter decomposers [13–15]. These studies revealed great diversity and evolutionary histories of viruses as well as new virus genome structures and virus lifestyles [16–18].

The International Committee for the Taxonomy of Viruses (ICTV) currently recognizes 23 families of mycoviruses, mostly comprising of linear double-stranded RNA (dsRNA), and positive-sense single-stranded RNA ((+)ssRNA). Recently, viruses with single-stranded circular DNA genomes

Received 02 August 2021; Accepted 01 October 2021; Published 01 December 2021

**Author affiliations:** <sup>1</sup>Atta-ur-Rahman School of Applied Biosciences (ASAB), National University of Sciences and Technology (NUST), H-12, 44000, Islamabad, Pakistan; <sup>2</sup>Institute of Plant Science and Resources, Okayama University, Kurashiki, 710-0046, Japan; <sup>3</sup>Crop Diseases Research Institute, National Agricultural Research Centre, Islamabad, Pakistan.

**\*Correspondence:** Muhammad Faraz Bhatti, mfbhatti@asab.nust.edu.pk

**Keywords:** screening; mycovirus; next-generation sequencing; *Fusarium mangiferae*; partitivirus; mitovirus; ourmiavirus.

**Abbreviations:** CBB, Coomassie Brilliant Blue; CDD, conserved domain database; dsRNA, double stranded RNA; *ef1α*, Elongation factor 1-alpha; FmVs, *F. mangiferae* viruses; ICTV, International Committee for the Taxonomy of Viruses; IGS, intergenic spacer; ITS, internal transcribed spacer; KPK, Khyber Pakhtunkhwa; NGS, next-generation sequencing; ORFs, open reading frames; PCR, polymerase chain reaction; PDA, potato dextrose agar; PEG, polyethylene glycol; RLM-RACE, RNA ligase-mediated rapid amplification of complementary cDNA ends; SDS-PAGE, SDS-polyacrylamide gel electrophoresis; ssRNA, single-stranded RNA; TEM, transmission electron microscope.

**†Present address:** Swiss Federal Institute for Forest, Snow and Landscape Research WSL, 8903 Birmensdorf, Switzerland

**§Present address:** EBS Universität für Wirtschaft und Recht, EBS Business School, Rheingaustrasse 1, 65375, Oestrich-Winkel, Germany. Accession numbers: MZ493897 to MZ493909.

**†**These authors contributed equally to this work

Four supplementary tables and eight supplementary figures are available with the online version of this article.

and negative-sense ssRNA ((-)ssRNA) genomes, whether segmented or non-segmented, have also been discovered [10, 19–23]. There will be an increasing number of taxa that accommodate mycoviruses year by year. The number and size of genome segments vary among mycoviral families. Many RNA mycoviruses may exist as multiple dsRNA elements in the genome of dsRNA viruses or in replicative form of ssRNA viruses (at least (+)ssRNA viruses). The electrophoretic profile with multiple dsRNA elements could be due to single infections by multipartite mycoviruses, multiple infections of mycoviruses or both, with or without subviral RNAs. Mixed infections of fungal isolates are commonly observed [12, 24]. For example, an isolate of *Fusarium poae* was reported to be infected by 16 RNA viruses belonging to 11 families [25], while an isolate of *Kickxella alabastrina* (the subdivision of Kickxellomycotina) was reported to be co-infected by 11 RNA viruses [14]. Other interesting cases are hypovirulent or a growth-retarded strain of the causal pathogen of Dutch elm disease (*Ophiostoma novo-ulmi*) or white root rot disease (*Rosellinia necatrix*) infected by multiple distinct viruses belonging to a single family [5, 26]. There seem to be complex virus/virus interactions such as co-infections (which have been intensively explored only in a limited number of cases). Known virus/virus interactions include synergism, antagonism, and mutualism [12, 27].

It should be noted that there is a bias in fungal sources in the aforementioned studies: some particular groups of fungi have been explored [14]. Ascomycetes, especially phytopathogenic ones, such as *Cryphonectria parasitica*, *Sclerotinia sclerotiorum*, *Rosellinia necatrix*, *Fusarium* spp., are screened much more extensively than others, because some of the mycoviruses in these fungi exhibit potential as viro-control (biocontrol of plant fungal diseases) agents [28–32]. There is also a bias in the locality of fungal sources. Until 2019, there had been no reports on fungal viruses from the Indian subcontinent. Recently, a few reports of mycoviruses are available from Pakistani fungal isolates, which includes complete characterization of three dsRNA viruses, *Alternaria alternata* victorivirus 1 (a novel victorivirus) [33], *Alternaria alternata* botybirnavirus 1 (AaBbV1, a novel botybirnavirus) [34, 35] and *Penicillium janthinellum* polymycovirus 1 (a strain of known polymycovirus) [36], and two strains of a novel polymyco-related (+)ssRNA virus, Hadaka virus 1–7 n and –1 NL (HadV1-7n and HadV1-1NL) [17]. In this study, a comprehensive screening was conducted during 2014 to 2019 for the identification of mycovirome (mycovirus populations) associated with Pakistani fungal isolates, and one of the infected isolates, *Fusarium mangiferae* (SP1), containing multiple mycoviral infections, was also characterized.

## METHODS

### Fungal strains isolation, identification and dsRNA extraction

A total of 396 samples (Fig. 1a–c) were collected from different areas of Pakistan, including provinces Punjab, Khyber Pakhtunkhwa (KPK), and the federal capital (Islamabad).

The sampling sites, years, and tentative species names of the 396 fungal isolates are available in Table S1 (available in the online version of this article). In water and soil samples, serial dilutions were used for culturing fungal strains on potato dextrose agar (PDA, Difco), while infected fruits and plant parts were cultured on PDA after surface sterilization with 1% sodium hypochlorite. The cultures on PDA were incubated at 25 °C for 5 to 7 days, followed by total nucleic acid and dsRNA extractions as described earlier [37, 38]. The nature of virus-specific nucleic acids was confirmed to be dsRNA via RQ1 DNase (Promega Corp.) and S1 Nuclease (Thermo Fisher Scientific Inc.) treatment. Glycerol stocks (40% v/v) of the pure colonies were prepared and stored at –80 °C for future use. All the fungal strains were subjected to morphological characterization through microscopy by observing the spore structure (under 40–100× magnification). Moreover, the virus-infected fungi were additionally subjected to PCR amplification of the internal transcribed spacer (ITS) of the ribosomal DNA [39]. Identification of fungal species was done both morphologically and molecularly through ITS sequencing (Figs S1 and S2, Table 1). Furthermore, for a particular fungal isolate, SP1, the elongation factor 1- $\alpha$  (*ef1 $\alpha$* ) and intergenic spacer (IGS) of the ribosomal DNA [40] were also amplified by PCR. Sequencing and phylogenetic analyses of IGS and *ef1 $\alpha$*  indicated that SP1 is a strain of the fungus belonging to *F. mangiferae* (Fig. S2).

### Next-generation sequencing of viral RNA elements

The viral genomes were sequenced using a combined approach of NGS and Sanger sequencing. Total RNA fractions were separately obtained from three dsRNA-positive fungal isolates, SP1 (*F. mangiferae*, a phytopathogen), L3 (*Diplodia seriata*, a phytopathogen), and HK (*Galactomyces candidum*, a soil-inhabitant) and were pooled (Table S2, Fig. S2) as a mixture of total RNAs (3.3  $\mu\text{g } \mu\text{l}^{-1}$ ). A ribosomal RNA (rRNA)-depleted RNA fraction was used for cDNA library construction using the TruSeq RNA Sample Preparation kit v2 (Illumina) and subsequent deep-sequencing with the Illumina HiSeq 2000 platform (Illumina, pair-end 100 bp reads) by Macrogen Inc. (Tokyo, Japan). After rRNA-depleted RNA-seq, a total of 41 889 108 reads were assembled into 42 770 contigs using the CLC Genomics Workbench (version 11, CLC Bio-Qiagen). These contigs were then subjected to local BLAST searches against the viral reference sequence (RefSeq) dataset of the National Centre for Biotechnology Information (NCBI). The virus-like contig sequences obtained from NGS were then confirmed by using one-step RT-PCR (PrimeScript one step RT-PCR kit, TaKaRa) or conventional RT-PCR and Sanger sequencing with their sequence-specific primers.

The terminal sequences were determined by the 3' RNA ligase-mediated rapid amplification of complementary cDNA ends (RLM-RACE) procedure as described by [34].

### Bioinformatic analysis

The viral and fungal nucleotide sequences were analysed using GENETYX DNA-processing software. NCBI ORF finder (<http://www.ncbi.nlm.nih.gov/gorf/gorf.html>) was

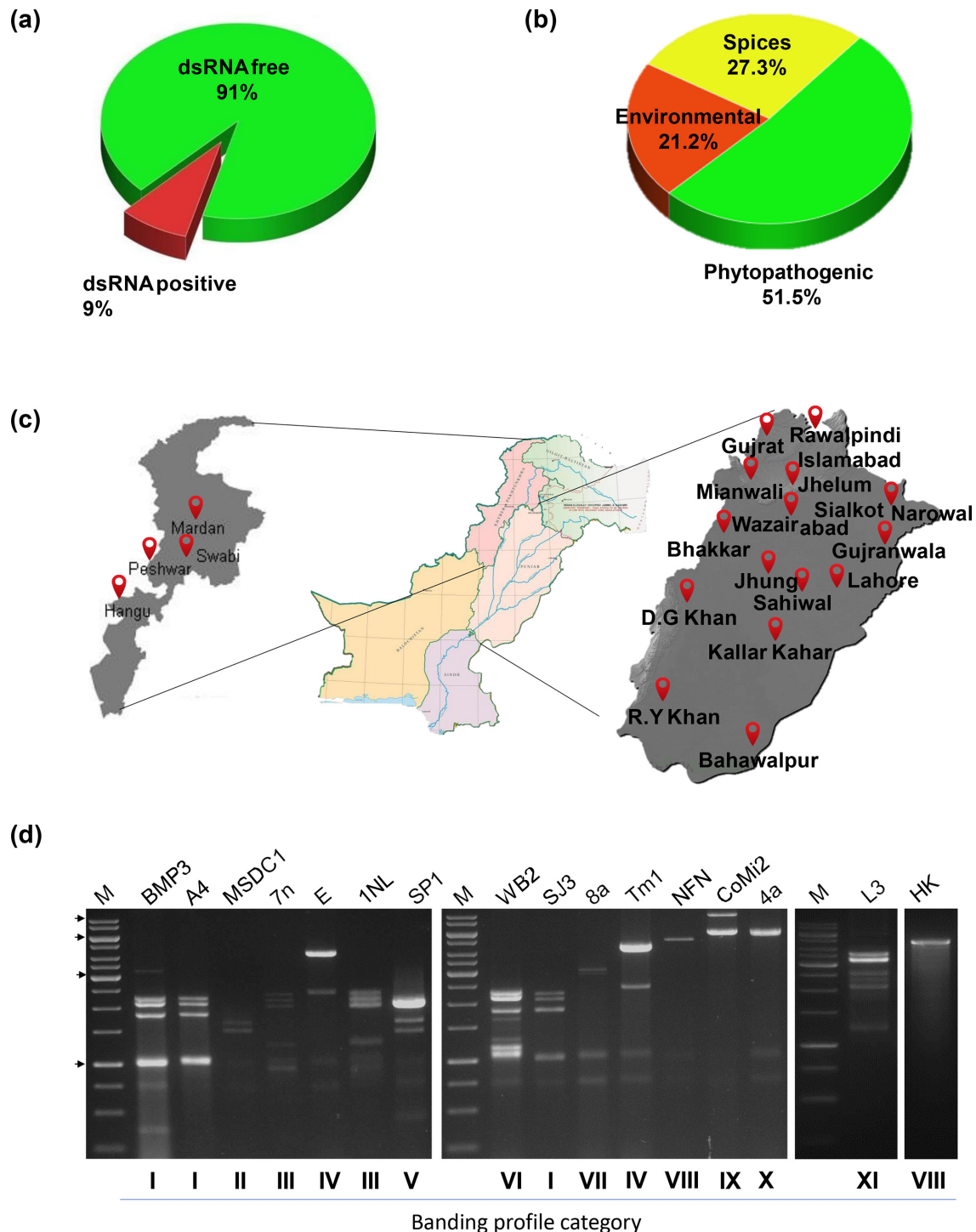


**Fig. 1.** Viruses detected from Pakistani fungal isolates. (a). Pie graph showing the percentage of dsRNA-positive screened fungal samples. (b). Graph showing the percentages of virus positive isolates collected from different sources. Spices samples include seeds, fruits, roots, barks, or other plant substance primarily used for flavouring or colouring food. Environmental samples include air, water and soil borne fungus. Phytopathogenic fungal samples were collected from diseased plants (c). Geographical distribution of collected samples. (d). Agarose gel electrophoresis of dsRNA extracted from pure mycelial cultures; 1% agarose gel was used for fractionation purpose. Fungal isolates: *Aspergillus niger*, BMP3; *Aspergillus fumigatus*, A4; *Aspergillus niger*, MSDC1; *Fusarium oxysporum*, 7n; *Geotrichum candidum*, E; *Fusarium nygami*, 1NL [35]; *Fusarium mangiferae*, SP1; *Penicillium oxalicum*, WB2; *Penicillium oxalicum*, SJ3; *Geotrichum candidum*, 8a; *Aspergillus fumigatus*, Tm-1; *Neofusicoccum parvum*, NFN; *Rhizopus oryzae*, CoMi2; *Alternaria alternata*, 4a [34]; *Diplodia seriata*, L3; *Galactomyces candidum*, HK. Labelling I-XII shows the categorization based on dsRNA profile.



used for the prediction of open reading frames (ORFs), with standard nuclear/cytosolic codon usage. For mitoviral candidates, yeast mitochondria codon usage was adopted as the deduction. Sequence similarity search was conducted by NCBI BLAST (BLASTn and BLASTx programmes) (<https://blast.ncbi.nlm.nih.gov/Blast.cgi>). NCBI conserved domain database (CDD) (<http://www.ncbi.nlm.nih.gov/Structure/cdd/wrpsb.cgi>) and motif finder (<https://www.genome.jp/tools/motif/>) were utilized for detecting conserved domains [41]. The virus sequence accession numbers were deposited in GenbankDDBJ/ENA database. The molecular mass of the protein encoded by viral genomes or their segments was calculated by an online protein molecular weight programme ([https://www.bioinformatics.org/sms/prot\\_mw.html](https://www.bioinformatics.org/sms/prot_mw.html)). The terminal secondary structure of both partitiviruses was predicted using the UNAFOLD Web Server (<http://www.unafold.org/mfold/applications/rna-folding-form.php>).

Phylogenetic analysis of the deduced protein sequences was performed by aligning the sequences using the online MAFFT server (version 7) (<https://mafft.cbrc.jp/alignment/server/>) [42]. The maximum-likelihood (ML) tree was generated using PhyML 3.0 with automatic model selection by SMS (Smart Model Selection) [43] (<http://www.atgc-montpellier.fr/phyml-sms/>). The ML tree was visualized using Figtree (version 1.4.4; <http://tree.bio.ed.ac.uk/software/>).

### Virus particles purification and SDS-PAGE

Mycelia (~30 g) was used to extract virus particles from isolate SP1. Particles were purified using a method described by [34]. The mycelia were ground into a fine powder using liquid nitrogen followed by the addition of 0.1 M phosphate buffer (pH 7.0), 0.1% (w/v) 2-mercaptoethanol, and two rounds of clarification with carbon tetrachloride (CCl<sub>4</sub>). The supernatant was mixed with 8% (w/v) polyethylene glycol (PEG-6000) and 1% (w/v) sodium chloride (NaCl) on ice with constant stirring for 2 h. Centrifugation was done (10 000 g) in 0.1 M phosphate buffer; insoluble particles were further eliminated by centrifugation (6000 g). The supernatant was overlaid onto a 20% sucrose cushion followed by ultracentrifugation (100 000 g) and subsequently fractionated with 20–50% (w/w) caesium chloride by ultracentrifugation (~150 000 g). Then 0.05 M phosphate buffer was used to dilute fractions containing particles, followed by ultracentrifugation (100 000 g). Pellets obtained during this process were re-suspended in 0.01 M phosphate buffer. Phenol:chloroform:isoamyl alcohol (25:24:1) extraction was used for nucleic acid isolation from particles. Extracted dsRNA was fractionated on 1% agarose gel, stained with ethidium bromide, and visualized under UV light.

Purified virus fractions were observed under the transmission electron microscope (TEM, model H-7650). Negatively straining with an alternative to uranyl acetate (EM stainer, Nissin EM Co.) was performed prior to the TEM observation. SDS-polyacrylamide gel electrophoresis (SDS-PAGE) was performed as described by [34], followed by Coomassie Brilliant Blue (CBB) staining.

## RESULTS

### Screening for the presence of mycoviruses

All 396 Pakistani fungal isolates collected from 2014 to 2019 (Table S1, Fig. 1c) were initially screened by a conventional dsRNA gel electrophoretic analysis for the presence of RNA mycoviruses. Consequently, 11 different dsRNA banding profiles (I–XI) were observed in 36 fungal isolates on agarose gel (Fig. 1d), suggesting these fungal isolates are infected with a particular RNA virus or viruses, and thus the minimal potential infection frequency [44] was estimated at ~9% among the tested fungal samples (Fig. 1a, b). The data of dsRNA-positive fungal samples is summarized in Table 1. The dsRNAs ranged in size from ~900 to 10 000 bp. The dsRNA patterns of 16 fungal isolates out of 36 dsRNA-positive ones are shown in Fig. 1(d), many of which show multiple bands. Several previously characterized fungal strains infected by RNA viruses were included in the dsRNA analysis as references, which included a botybirnavirus (AaBbV1)-infected *Alternaria alternata* isolate 4 a [34], a hadakavirus (HadV1-7n)-infected *Fusarium oxysporum* isolate 7 n and a HadV1-1NL infected *Fusarium nygami* isolate 1 NL [17, 35] (Fig. S2). We subjected three dsRNA-positive fungal isolates, SP1 (*F. mangiferae*, phytopathogen, collected from a potato plant in Hangu, 2018) (Fig. 2a), L3 (*Diplodia seriata*, phytopathogen, collected from *Lokath* in Kallar Kahar, 2018), and HK (*Galactomyces candidum*, soil-inhabitant, collected from a tomato plant in Islamabad, 2016) to NGS (Tables 1 and S1, Fig. S2).

A total of 22 virus-like contigs were detectable in the three fungal strains that included contigs with similarity to dsRNA viruses (chrysovirus, totivirids, polymycovirus, partitivirids) and (+)ssRNA viruses (narnavirids, mitovirids, botourmiavirids). We first investigated by one-step RT-PCR with contig-specific primer sets which fungal strain harboured NGS-detected virus-related sequences. The virus-like contig-fungal strain assignment is shown in Table S2.

### Mycoviruses from *Fusarium mangiferae* isolate SP1

This study focused on the fungal strain *F. mangiferae* SP1 that turned out to be co-infected by 11 RNA viruses (Table S2). The characterization of other viruses carried in the other two fungal strains (L3 and HK) will be reported elsewhere. The dsRNA profile of isolate SP1 showed the presence of dsRNA ranging from 1.6 kbp to 2.4 kbp (two major and two minor dsRNA bands) (Figs 1d and 2b). However, NGS results revealed multiple virus infections of the SP1 strain. The virus-like contig sequences showed sequence similarity to mitovirids, botourmiavirids (phylum *Lenarviricota*) and partitivirids (phylum *Pisuviricota*) (Table S2 and see below). RT-PCR with primers designed from assembled contigs of NGS data (Table S3) validated the presence of eleven viruses (two partitivirids, six mitovirids and three botourmiavirids) in strain SP1 (Fig. 2c). No RT-PCR fragments were obtained from the L3 and HK fungal strains by using these primer sets (data not shown). The BlastP and BlastX results of identified mycoviral sequences are mentioned in Tables 2 and S4. The genome organization of these viruses is represented in Figs 3a

**Table 1.** Environmental isolates of fungi infected with their source and respective mycoviral infection.

Sr. No.†	Isolate	Profile category†	Source	Infected fungi/Host
	BPM3	I	Black pepper	<i>Aspergillus niger</i>
	A4	I	Air	<i>Aspergillus fumigatus</i>
	MSDC1	II	Mango	<i>Aspergillus niger</i>
	7n	III	Tomato	<i>Fusarium oxysporum</i>
	E	IV	Mushroom	<i>Geotrichum candidum</i>
	1NL	III	Pomegranate	<i>Fusarium nygami</i>
	SP1	V	Potato	<i>Fusarium mangiferae</i>
	WB2	VI	Water	<i>Penicillium oxalicum</i>
	SJ3	I	Soil	<i>Penicillium oxalicum</i>
	8a	VII	Tomato	<i>Geotrichum candidum</i>
	Tm-1	IV	Tomato	<i>Aspergillus fumigatus</i>
	NFN	VIII	Banana	<i>Neofusicoccum parvum</i>
	CoMi2	IX	Coriander	<i>Rhizopus oryzae</i>
	4 a	X	Tomato	<i>Alternaria alternata</i>
	L3	XI	Loquat	<i>Diplodia seriata</i>
	HK	VIII	Tomato	<i>Galactomyces candidum</i>
	LI19C3	VIII	Milk sample	<i>Aspergillus fumigatus</i>
	9a	VIII	Tomato	<i>Botrytis spp.</i>
	SJ5	IV	Soil	<i>Penicillium oxalicum</i>
	BPM6	I	Black pepper	<i>Aspergillus niger</i>
	SSP2	VIII	Tomato	<i>Fusarium graminearum</i>
	A6	I	Air	<i>Aspergillus fumigatus</i>
	A8	VIII	Soil	<i>Trichoderma longibrachiatum</i>
	A23	V	Air	<i>Aspergillus fumigatus</i>

Continued

Table 1. Continued

Sr. No.*	Isolate	Profile category†	Source	Infected fungi/Host
	BP1	I	Black pepper	<i>Aspergillus fumigatus</i>
	Ca1	I	Cardamom	<i>Aspergillus fumigatus</i>
	Co5	I	Coriander	<i>Aspergillus fumigatus</i>
	Cu4	IV	Cumin	<i>Rhizopus oryzae</i>
	FG1	I	Fenugreek	<i>Aspergillus fumigatus</i>
	Gr-1	I	Grapes	<i>Aspergillus fumigatus</i>
	Gr-2	I	Grapes	<i>Aspergillus fumigatus</i>
	Gr-3	I	Grapes	<i>Aspergillus fumigatus</i>
	K1	X	Nigella	<i>Rhizopus oryzae</i>
	OnJ3	I	Onion	<i>Aspergillus fumigatus</i>
	PM3	IX	Peppermint	<i>Rhizopus oryzae</i>
	SR3	I	Soil	<i>Aspergillus fumigatus</i>

\*Each row shows a serial number assigned to the dsRNA.

†Mycoviruses have been assigned to category based on their dsRNA profile patterns (see Fig. 1d for representative fungal strains)

and 5a. The characteristics of the 11 viruses carried in strain SP1 are described below. The 5'- and 3'-terminal sequences of each RNA virus were determined by Sanger sequencing of three to five RACE clones obtained from each terminus. The sequences of primers used in RACE are shown in Table S3.

### Characterization of two partitivirids

NGS data analysis revealed four partitivirus-related contigs (61, 112, 145, and 423) (Tables 2 and S4: two with similarity to partitivirus RNA-dependent RNA polymerase (RdRP) and two resembling partitivirus coat protein (CP). These contigs were assumed to represent two partitivirids, likely a member of the genus *Betapartitivirus* (contigs 423 and 145) and a member of *Gammapartitivirus* (contigs 112 and 61), based on their sequence similarity to other members of the respective genera. To cover the whole genome of these segments, we conducted RACE and RT-PCR with Sanger sequencing by using total RNA fractions of *F. mangiferae* SP1. The betapartitivirus and gammapartitivirus were tentatively named as *Fusarium mangiferae* partitivirus 1 (FmPV1) and *Fusarium mangiferae* partitivirus 2 (FmPV2). The larger segment dsRNA1 of FmPV1 comprised 2345 bp containing an open reading frame that would encode 715

amino acids (RdRP) with a molecular mass of ~83.7 kDa. DsRNA2 of FmPV1 comprising 2195 bp encodes an ORF encoding 629 amino acids (CP) with an anticipated molecular mass of ~70.8 kDa (Fig. 3a). FmPV1 RdRP showed the highest amino acid identity to *Plasmopara viticola* lesion associated partitivirus 7 RdRP (58.67%), while FmPV1 CP shared the highest amino acid identity (53.35%) with *Neurospora discreta* partitivirus 4 (Tables 2 and S4). While dsRNA1 (RdRP) and dsRNA2 (CP) of FmPV2 comprised 1772 bp and 1571 bp encoding 539 amino acids (RdRP, molecular mass ~62.99 kDa) and 410 amino acids (CP, molecular mass ~44.6 kDa), respectively (Fig. 3a). The highest amino acid sequence identity was detected between FmPV2 RdRP and *Metarhizium brunneum* partitivirus 2 RdRP (85.34%) and between FmPV2 CP and *Colletotrichum partitivirus* 1 CP (68.26%) (Tables 2 and S4). RdRP amino acid sequence alignment of both partitivirids with other recognized viruses from family *Partitiviridae* identified several conserved domains (domains A–F; Fig. S3) as previously described by [45]. The motif G is not conserved within the members of the family *Partitiviridae* [46], and the same was observed for the two viruses under investigation. At the N terminal region (near motif F), a conserved glycine

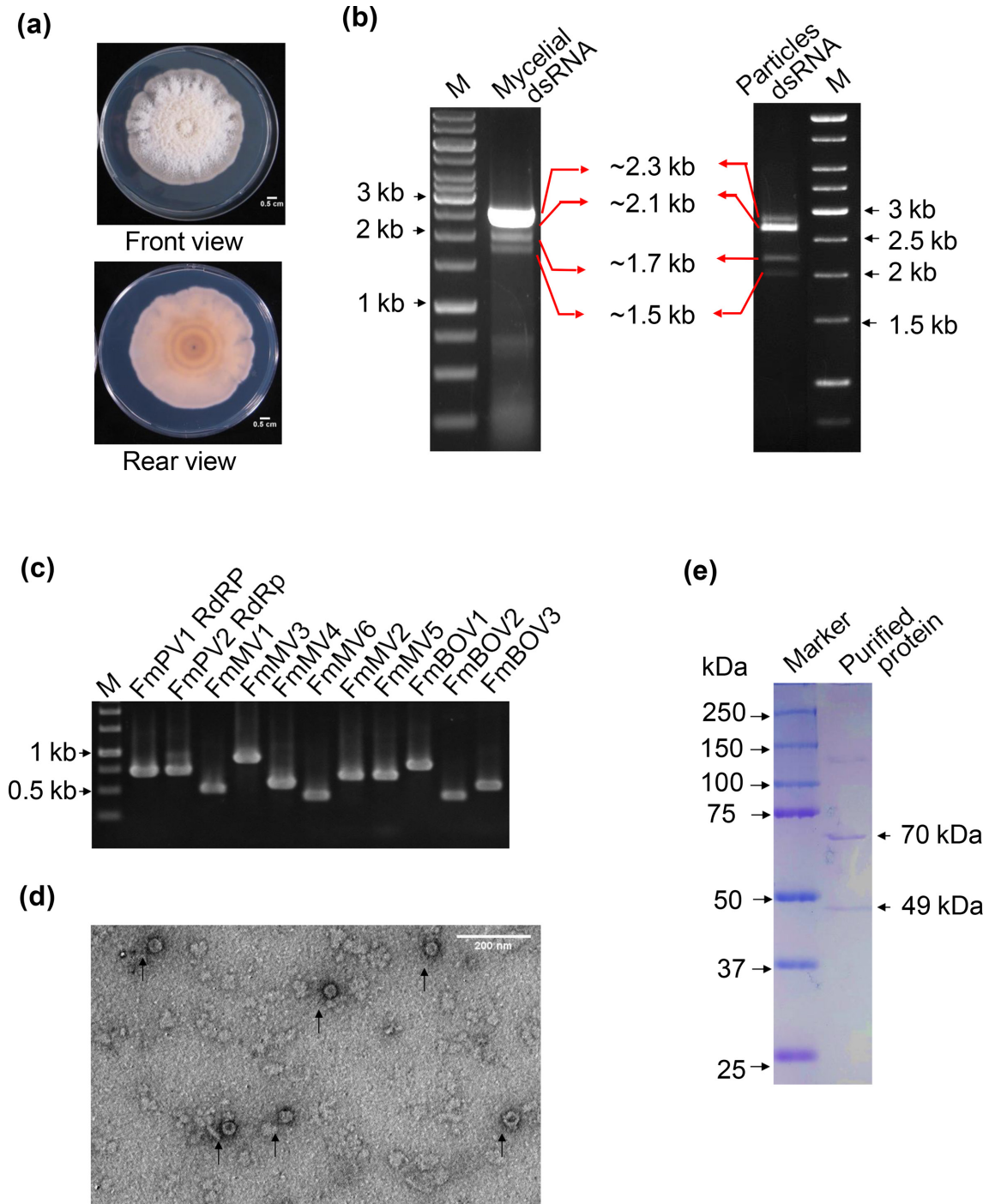


**Fig. 2.** (a). *Fusarium mangiferae* isolate SP1 (front and rear view) harbouring encapsidated partitivirids, along with capsidless mitovirids and botourmiavirids. (b) Agarose gel profile picture showing the presence of dsRNA of putative mycoviruses (left pane shows mycelial dsRNA, Right pane shows dsRNA from purified particles). (c) RT-PCR confirmation of all the viruses present in isolate SP1. The putative viruses were tentatively named: *Fusarium mangiferae* partitivirus 1 and 2, FmPV1 and FmPV2; *Fusarium mangiferae* mitovirus 1 to 6, FmMV1 to FmMV6; *Fusarium mangiferae* botourmiavirus 1 to 3, FmBOV1 to FmBOV3. (d) Electron microscopy of a virion enriched fraction extracted from isolate SP1. Hitachi electron microscope model H-7650 was used to examine purified virus preparations. Bar represents 200 nm. (e). SDS-PAGE analysis was performed using purified virus preparation in 10% gel. Precision plus protein dual colour standards (BioRad) was used as marker.

**Table 2.** BLASTp results of RdRP amino acid identity of members of the phyla Lenarviricota.

Virus name	Contig no.	Segments	Identity (%)	Cover (%)	BLASTp	Accession
FmPV1	423	dsRNA1	58.67	98	Plasmopara viticola lesion associated	QHD64796.1
	145	dsRNA2	53.35	98	Partitivirus 7 Neurospora discrete partitivirus 4	BCL64203.1
FmPV2	112	dsRNA1	85.34	100	Metarhizium brunneum partitivirus	QTC11257.1
	61	dsRNA2	68.26	96	2 Colletotrichum partitivirus 1	QTC11258.1
FmMV1	33	Non-segmented	72.21	98	Soybean leaf-associated mitovirus 1	ALM62241.1
FmMV2	69	Non-segmented	86.86	100	Fusarium oxysporum mitovirus 1	QTV99352.1
FmMV3	7	Non-segmented	69.17	100	Plasmopara viticola lesion associated mitovirus 24	QIR30247.1
FmMV4	74	Non-segmented	84.68	100	Fusarium globosum mitovirus 1	YP_009126872.1
FmMV5	16	Non-segmented	68.20	97	Plasmopara viticola lesion associated mitovirus 46	QIR30269.1
FmMV6	25	Non-segmented	68.13	100	Fusarium poae mitovirus 1	YP_009272898.1
FmBOV1	419	Non-segmented	81.25	100	Fusarium oxysporum ourmia-like virus	QPO14979.1
FmBOV2	47	Non-segmented	73.20	100	Plasmopara viticola lesion associated ourmia- like virus 44	QGY72574.1
FmBOV3	9	Non-segmented	40.14	76	Penicillium citrinum ourmia-like virus 1	AYP71797.1

residue was observed, which can be considered as motif G [46]. A highly conserved GDD motif was also observed in the RdRP of both viruses (Fig. S3). Like the previously reported partitiviruses, FmPV1 exhibited similar features in their terminal sequences [47, 48], and out of 20 nucleotides located at the 5' termini of both the segments, 19 were identical, that included 5'-AGAAUU...-3', as observed in other betapartitiviruses including Rosellinia necatrix partitivirus 1 [49] (Fig. S4). The 5' end of the plus strands of FmPV2 dsRNA1 and dsRNA2 is the hepta-nucleotide 5'-CGCAAAA...-3', as in the case for many other gamma-partitiviruses (Fig. S4). The positive strands of the FmPV1 genomic dsRNAs have an interrupted poly(A) tail at the 3' termini, while no interrupted poly(A) tail was found in those of the FmPV2 genomic dsRNAs, which is a feature of gammapartitiviruses [47, 50, 51] (Fig. S4). Predicted secondary structures of both FpMV1 and 2 showed the presence of stem loop and pan handle like structures at 5' and 3' terminals (Fig. S5).

The complete nucleotide sequence of dsRNA1 of both FmPV1 and FmPV2 has been deposited in the GenBank/ DDBJ/ENA database with the accession numbers

MZ493897, MZ493899 and dsRNA2 sequences with accession MZ493898 and MZ493900, respectively.

Phylogenetic analysis, based on RdRP of FmPV1 and FmPV2 as well as selected partitiviruses from all the genera of the family *Partitiviridae*, showed that FmPV1 clustered with betapartitiviruses with a bootstrap branch support value of 99, while FmPV2 clustered and nested with gammapartitiviruses with a moderate branch support value of 100 (Fig. 3b). This result was in accordance with the BlastP search with FmPV1 and FmPV2 RdRP, showing high similarity scores to betapartitiviruses and gammapartitiviruses, respectively.

TEM observations revealed spherical particles with a diameter of 30–40 nm in the purified virus fractions from the *F. mangiferae* SP1 strain (Fig. 2d, arrowheads). The protein components of virion preparations were analysed by SDS-PAGE, which showed two major protein bands of 70 and 49 kDa. The 70 and 49 kDa proteins likely represent FmPV1 and FmPV2 CPs, respectively, from the coding capacity deduced from the nucleotide sequences of FmPV1 and FmPV2 dsRNA2s (Fig. 2e, arrowheads). Thus, the purified



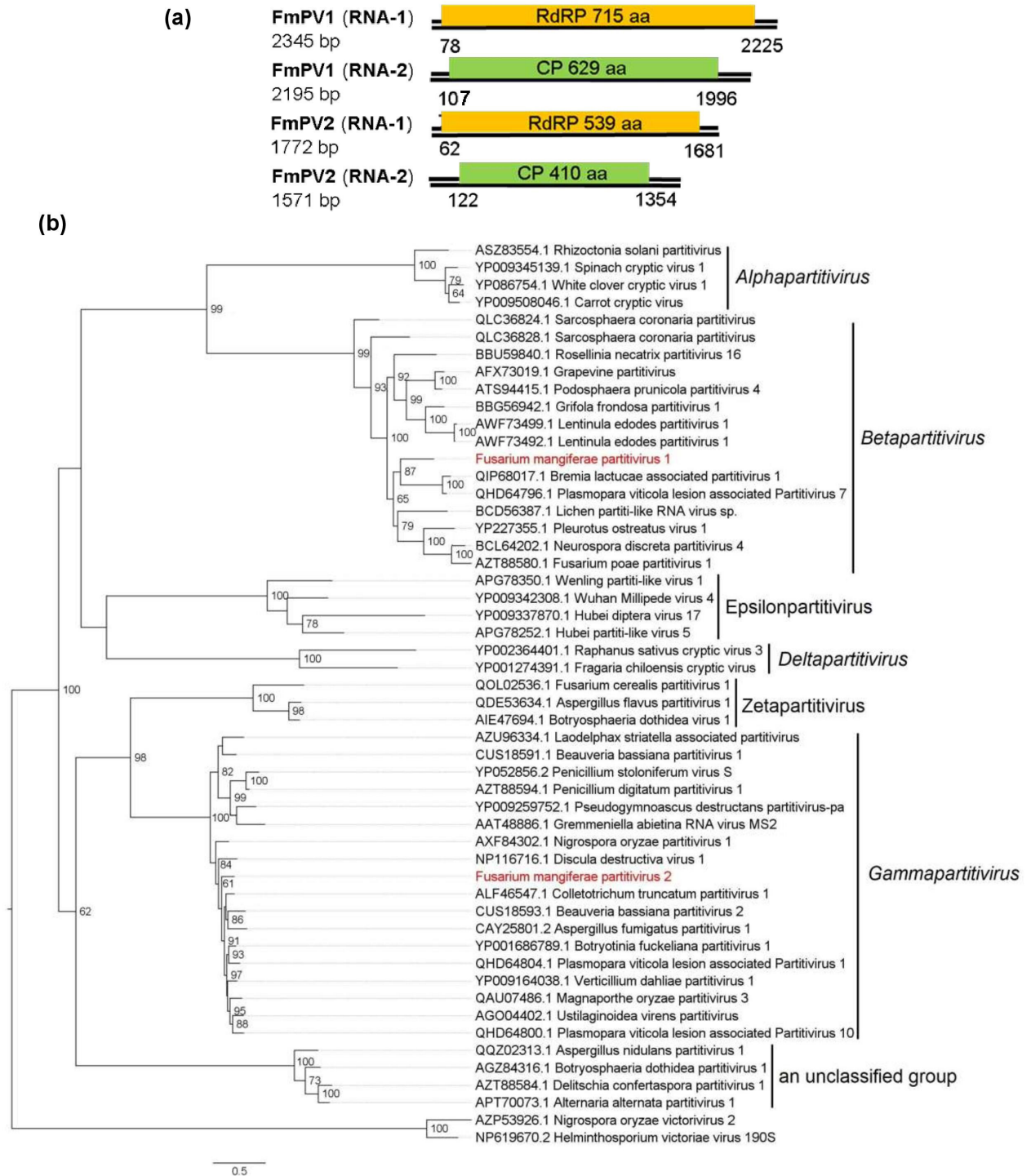


**Fig. 3.** (a) Schematic representation of two partitiviruses, *Fusarium mangiferae* partitivirus 1 and 2 (FmPV1 and FmPV2), identified in *F. mangiferae* isolate SP1 (a betapartitivirus, FmPV1 and a gammapartitivirus, FmPV2). The RdRP segments are represented in yellow and CP segments are represented in green. (b) Phylogenetic analysis based on RNA-dependent RNA polymerase of FmPV1 and FmPV2. Tree was derived using maximum-likelihood method with amino acid alignments of the deduced ORFs. Numbers at the nodes are bootstrap values in percent out of 1000 replicates. Bootstrap values less than 60 are not shown. The members of family *Totiviridae* (victoriviruses) are used as outgroups to root the tree.

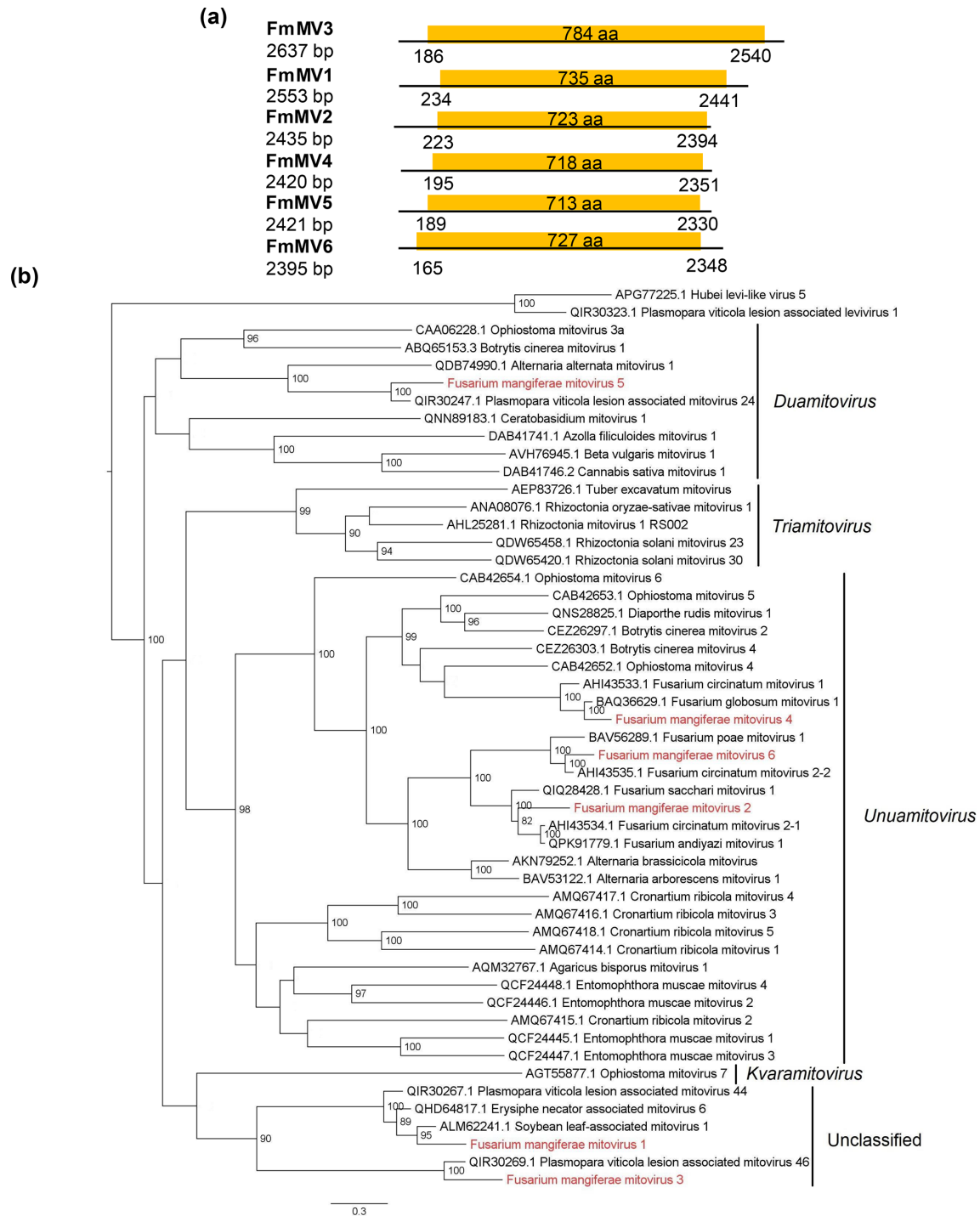


**Fig. 4.** (a) Schematic representation of six mitovirids, *Fusarium mangiferae* mitovirus 1 to 6 (FmMV1 to FmMV6), identified in *F. mangiferae* isolate SP1 (*Unuamitovirus*, *Duamitovirus* and unclassified mitovirids). ORFs regions are shown as yellow. (b) Phylogenetic analysis based on RNA-dependent RNA polymerase of FmMV1 to FmMV6. Tree was made using maximum-likelihood method with amino acid alignments of the deduced ORFs. Numbers at the nodes are bootstrap values in percent out of 1000 replicates. Leviviruses (family *Leviviridae*) are used as outgroups to root the tree. Bootstrap values less than 70 are not shown.

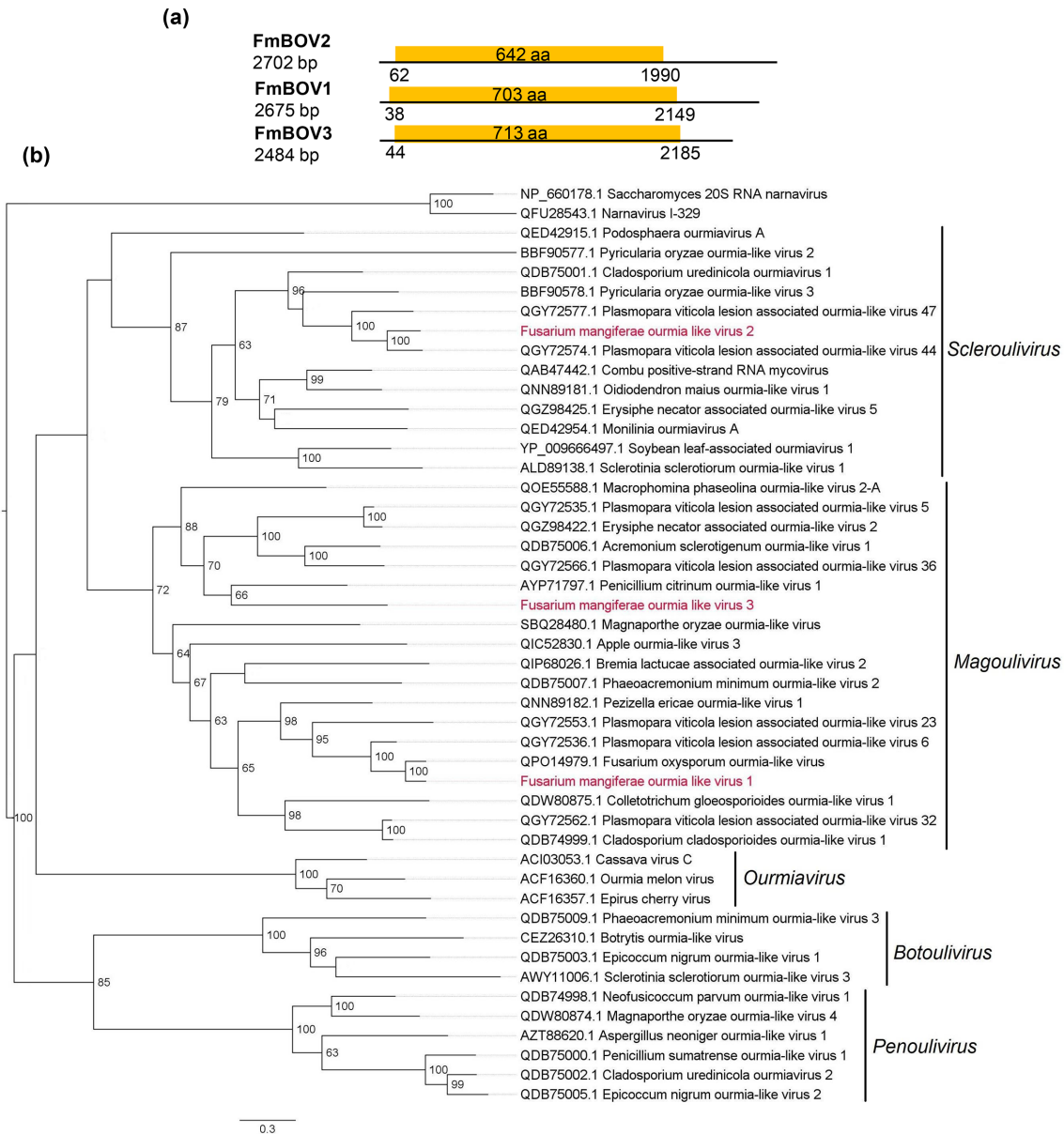


**Fig. 5.** (a) Schematic representation of three botourmiavirids, *Fusarium mangiferae* botourmiavirus 1 to 3 (FmBOV1 to FmBOV3), identified in *F. mangiferae* isolate SP1 (*Magoulivirus* and *Scleroulivirus*). The ORF regions are shown as yellow. (b) Phylogenetic analysis based on RNA-dependent RNA polymerase of FmBOV1 to FmBOV3. The tree was made using maximum-likelihood method with amino acid alignments of the deduced ORFs. Numbers at the nodes are bootstrap values in percent out of 1000 replicates. Bootstrap values less than 60 are not shown. Members of the family *Narnaviridae* (narnaviruses) are used as outgroups to root the tree.

particle fractions were considered to contain a mixture of FmPV1 and FmPV2. The dsRNA profile in a purified fraction was similar to that obtained from SP1 mycelia. A minor upper band (2.3 kbp) which is likely corresponded to FmPV1 dsRNA1. (Fig. 2b). Virion transfection of *Cryphonectria parasitica* allowed for the isolation of transfectants singly infected by FmPV1, that carried only the larger dsRNA segments of ~2.3 kbp and ~2.2 kbp, and transfectants doubly infected by FmPV1 and FmPV2 (H. A. Khan and N. Suzuki, unpublished results). This suggests that

the genome segment assignment of FmPV1 and FmPV2 is correct.

### Genomic sequences of mitovirids

Six virus-like contigs in the NGS data showed sequence similarity to previously reported mitovirids (Tables 2 and S4). Their entire genome sequences were obtained via RACE and RT-PCR with Sanger sequencing by using total RNA samples of *F. mangiferae* SP1. The predicted viruses were

tentatively named *Fusarium mangiferae* mitovirus 1 to 6 (FmMV1 to FmMV6), respectively. The dsRNA of these viruses was not visible on agarose gel, possibly because of low-level accumulation of replicative form dsRNA, but their viral RNA was readily detected by RT-PCR and NGS (Fig. 2c, Table 2). No clear sequence conservation was found at the 5' and 3' terminal sequences between the identified mitovirids or known ones. The sizes of these viruses range from 2637 to 2395 nt with single long ORFs that are detected when the mitochondrial codon usage is applied. The sizes in amino acids of RdRPs encoded by FmMV1 to FmMV6 were 735, 723, 784, 718, 713, and 727, respectively. All the mitovirids (FmMV1 to FmMV6) isolated shared the signature RdRP domain (Mitovir\_RNA\_pol, pfam05919). Multiple amino acid sequence alignment of RdRP from these mitovirids with other known mitovirids showed the presence of six conserved motifs [45, 52] that are characteristic of mitovirids. A conserved GDD motif was also observed in all aligned sequences (Fig. S6). The RdRPs of FmMV1 to FmMV6 shared 72.21, 86.86, 69.17, 84.68, 68.20, and 68.13% amino acid sequence similarity with previously reported Soybean leaf-associated mitovirus 1 (unclassified), *Fusarium oxysporum* mitovirus 1 (*Unuamitovirus*), *Plasmopara viticola* lesion associated mitovirus 24 (*Duamitovirus*), *Fusarium globosum* mitovirus 1 (*Unuamitovirus*), *Plasmopara viticola* lesion associated mitovirus 46 (unclassified), and *Fusarium poae* mitovirus 1 (FpMV1) (*Unuamitovirus*), respectively (Tables 2 and S4). Low amino acid sequence similarity between these mitovirids showed un-relatedness and independent replication of these viruses (Fig. S7).

Phylogenetic analysis, based on the deduced amino acid sequence of RdRP, revealed that all the six mitovirids belongs to the family *Mitoviridae* (Fig. 4b). FmMV1 and 3 made a clade with unclassified mitovirids. FmMV2, 4 and 6 made a clade with the members of the genus *Unuamitovirus*, while FmMV5 falls with *duamitoviruses* in the family *Mitoviridae*.

Complete nucleotide sequences of FmMV1 to FmMV6 have been submitted in GenBank/DDBJ/ENA with accession numbers MZ493901, MZ493902, MZ493903, MZ493904, MZ493905, and MZ493906, respectively.

### Genomic sequences of botourmiavirids

Three botourmia-like virus contigs were also detected in the isolate SP1. Like the mitovirids, no replicative form dsRNA derived from botourmia-like viruses appeared to be detected on agarose gel, although their presence was confirmed through RT-PCR in the *F. mangiferae* SP1 strain (Fig. 2c). They were tentatively named as *Fusarium mangiferae* botourmiavirus 1, 2, and 3 (FmBOV1 to FmBOV3). FmBOV1 to FmBOV3 showed a coding-complete genome with a size of 2685, 2712, and 2517 nt possessing single ORFs that would encode RdRPs of 703, 642, and 713 amino acids, respectively (Fig. 5a). These RdRPs show sequence identity of 81.25, 73.20 and 40.14% to known botourmiavirids such as *Fusarium oxysporum* ourmia-like virus, *Plasmopara viticola* lesion associated ourmia-like virus 44 and *Penicillium citrinum* ourmia-like

virus 1, respectively (Tables 2 and S4). FmBOV1–3 shared eight conserved motifs with other reported botourmiaviruses (Fig. S8). Phylogenetically, these viruses were clustered with previously reported botourmia and botourmia-like viruses with high and moderate branch support values 87% for *scleroulivirus* and 72% for *magoulivirus*, respectively (Fig. 5b). The family *Botourmiaviridae* was established in 2018 and now includes four genera: *Ourmiavirus* (plant viruses), *Botoulivirus*, *Magoulivirus*, and *Scleroulivirus* (fungal viruses) [53].

Nucleotide sequences of FmBOV1 to FmBOV3 have been submitted in GenBank/DDBJ/ENA database with MZ493907, MZ493908 and MZ493909 accessions, respectively.

## DISCUSSION

This study represents a large-scale screening of 396 diverse fungal isolates for viruses for the first time in the Indian subcontinent. We used a classical dsRNA agarose gel electrophoresis method and showed a modest (9%) incidence rate (36/396). This value may underestimate the actual virus infection rate as some of the mycoviruses may go undetected because of lower concentration or co-migration which is beyond the level of resolution for agarose gel electrophoresis method [54]. Of 36, three fungal isolates were subjected to NGS (Table S2). We focused only on one isolate, SP1, of the phytopathogenic fungus *Fusarium mangiferae*, isolated from a potato. This fungal strain was shown to be co-infected by 11 mycoviruses: two partitivirids, three botourmiavirids, and six mitovirids. Of note, the 11 viruses detected from one fungal strain all belong to 11 new species (Fig. 2c). This observation supports the notion that *F. mangiferae* has not been explored as a virus-host, although other *Fusarium spp.* has been reported to host many viruses [32, 55]. Mixed infection of fungi by a few viruses is commonly observed [12]. The number of coinfecting viruses, 11, in SP1 is among the largest. Other such examples were reported from a basidiomycete (*Rhizoctonia solani*) and an ascomycete (*F. poae*) were coinfecting by 17 and 16 viruses [25, 45]. There may be unexplored virus/virus interactions in SP1, as in the case of other co-infections [12, 56]. Further analysis is required to confirm the biological roles and interactions of these viruses with each other. Importantly, almost half of the sequenced viruses (seven viruses) should be described as new taxa at the species level, as discussed below (see also Table S2).

Of the 11, only two partitivirids, FmPV1 and FmPV2, are encapsidated dsRNA viruses (Fig. 2d,e). Phylogenetic analysis with RdRP showed FmPV1 and FmPV2 to have an affinity to betapartitiviruses and gammapartitiviruses (Fig. 3b). The species demarcation criteria set by ICTV for partitivirids are  $\leq 90\%$  aa sequence identity at the RdRP level and  $\leq 80\%$  protein identity at the CP level [47, 48]. FmPV1 and FmPV2 showed sequence identity to other reported partitiviruses (Table 2). These simultaneously meet the ICTV criteria, indicating that each virus belongs to a novel species within the genus *Betapartitivirus* or *Gammapartitivirus*. Gammapartitiviruses have been reported only in ascomycetes thus far [47, 48], while betapartitiviruses infect either plants or fungi



and their ancestors are assumed to have been transferred between the two kingdoms [57, 58]. Although both viruses belong to the family *Partitiviridae* (phylum *Pisuviricota*), they show different molecular features [47]. As noted earlier, FmPV1 and FmPV2 were differentiated in segment size, presence or absence of an interrupted poly(A) tract and conserved 5'-terminal sequence (Figs 2b and 3a and S4).

Co-infection by multiple partitivirids alone or with other mycoviruses has also been reported previously in many isolates, including *R. necatrix* strains. *R. necatrix* strain W442 is one example that harbours a betapartitivirus (Rosellinia necatrix partitivirus 18) and an alphapartitivirus (Rosellinia necatrix partitivirus 19) belonging to *Betapartitivirus* and *Alphapartitivirus* that show different inducing levels of antiviral RNA silencing [5, 59]. Also reported is the involvement of partitivirids in hypovirulence of phytopathogenic fungal strains co-infected with viruses from other families [27, 60, 61]. Partitivirids are among the transfectable encapsidated dsRNA fungal viruses [61–67]. Transfection protocols available for partitivirids should be helpful to clarify the possible phenotypic effects of FmPV1 and FmPV2 on the host fungus, *F. mangiferae*.

For mitovirids and botourmiavirids, the species demarcation criteria are <70 and <90% RdRP sequence identity, respectively [53, 68]. The six newly detected mitovirids share over 68–84% of RdRP sequences with previously reported viruses. For example, FmMV4 and FmMV6 show 84.68 and 68.13% RdRP sequence identities to *Fusarium globosum* mitovirus one and FpMV1, which have been proposed to represent the species *Unuamitovirus fugl1* and *Unuamitovirus fuox1*, respectively. The other mitovirids (FmMV1–3, FmMV5) of *F. mangiferae* also show the highest RdRP sequence identity to unassigned mitovirids. The three newly characterized botourmiavirids meet the species criteria and thus belong to new species. Mitovirids and botourmiavirids belong to the phylum *Lenarviricota* and commonly have a capsidless nature with the simplest mono-segmented (+)ssRNA genome encoding only RdRP [69]. Similarities extend to relatively frequent coinfections. Infection of single host fungi by multiple mitovirids or botourmiavirids has been seen in many fungal isolates previously [45, 70–72]. Notably, seven mitovirids belonging to seven independent species have been previously reported to infect a hypovirulent isolate of *O. novo-ulmi* [26, 73]. Similarly, a single *Magnaporthe oryzae* isolate was reported to be co-infected by four botourmiavirids [74]. This study revealed the simultaneous co-infection by six mitovirids (FmMV1 to FmMV6) and three botourmiavirids (FmBOV1 to FmBOV3). It is not so common that a single host organism is multiply infected with members of a single family, because cross-protection or interference against each other may happen. No evidence is available for host RNA silencing targeting mitovirids, while small RNAs appear to be generated in infected cells [75–77]. These mitovirids show 21–44% nucleotide sequence identity to each other. Thus, there would not be RNA-silencing mediated interference between the six mitovirids, even if RNA silencing targets mitovirids. On the other hand, botourmiavirids are targeted

by host antiviral RNA silencing [78]. It seems that the three co-infecting botourmiavirids are divergent enough to evade antiviral RNA silencing inducing cross-protection.

Fungal mitovirids and botourmiavirids, members of the families *Mitoviridae* and *Botourmiaviridae*, are readily distinguishable phylogenetically and biologically [53]. Mitovirids are assumed to have originated from bacterial phages and to have coevolved with mitochondria since alphaproteobacteria became endosymbionts of eukaryotes. Mitovirids are replicated in the mitochondria and use the mitochondrial genetic code for translation, typically UGA, to encode tryptophan. Many of their properties remain to be explored [12, 75]. They have been co-purified together with mitochondria [79]. Fungal botourmiavirids, on the other hand, appear to replicate in the cytoplasm as in the case of plant botourmiavirids (ourmiaviruses) [53, 80], although no direct evidence is available. This notion is supported by the observation that transfection of fungal host protoplasts by *in vitro* synthesized viral transcripts from the full-length cDNA leads to the establishment of infection [81]. This would not be possible if fungal botourmiavirids were replicated in the mitochondria.

#### Funding information

This investigation was partly supported by HEC grant (No: PM-IPFP/HRD/HEC/2012/2718 awarded to MFB and NV) and NUST students research, Grants-in-Aid for Scientific Research (A) and Grants-in-Aid for Scientific Research on Innovative Areas from the Japanese Ministry of Education, Culture, Sports, Science and Technology (KAKENHI 21H05035, 17H01463, 16H06436, 16H06429 and 16K21723 to N.S and H.K.).

#### Acknowledgements

The authors are grateful to Ms Sakae Hisano and Dr Paul Telengech for technical assistance. HAK is thankful to the Higher Education Commission (HEC) of Pakistan for fellowship under the International Research Support Initiative Programme (IRSIP).

#### Authors and contributors

H.A.K., and W.S.: Investigation, writing - original draft. M.J., M.S., T.F., A.A., M.A., M.W., S.B., and M.M.D.: Investigation. A.J., and H.K., Investigation, results interpretation, reviewing and editing original draft. N.V., and H.A.J.: Assisted in sample acquisition, reviewing and editing of original draft. M.F.B., and N.S.: Conceptualization, Supervision, results interpretation, Writing - reviewing and editing- original draft.

#### Conflicts of interest

The authors declare that there are no conflicts of interest.

#### Ethical statement

This article does not contain any studies with human participants or animals performed by any of the authors.

#### References

1. Kondo H, Hisano S, Chiba S, Maruyama K, Andika IB, et al. Sequence and phylogenetic analyses of novel totivirus-like double-stranded RNAs from field-collected powdery mildew fungi. *Virus Res* 2016;213:353–364.
2. Marzano SYL, Domier LL. Novel mycoviruses discovered from metatranscriptomics survey of soybean phyllosphere phytobionts. *Virus Res* 2016;213:332–342.
3. Nerva L, Forgia M, Ciuffo M, Chitarra W, Chiappello M, et al. The mycovirome of a fungal collection from the sea cucumber *Holothuria polii*. *Virus Res* 2019;273:197737.
4. Koonin EV, Dolja VV. Metaviromics: a tectonic shift in understanding virus evolution. *Virus Res* 2018;246:A1–a3.

5. Telengech P, Hisano S, Mugambi C, Hyodo K, Arjona-López JM, et al. Diverse partitiviruses from the phytopathogenic fungus, *Rosellinia necatrix*. *Front Microbiol* 2020;11:1064.
6. Chiapello M, Rodríguez-Romero J, Ayllón MA, Turina M. Analysis of the virome associated to grapevine downy mildew lesions reveals new mycovirus lineages. *Virus Evol* 2020;6:veaa058.
7. Chiba Y, Oiki S, Yaguchi T, Urayama SI, Hagiwara D. Discovery of divided RdRp sequences and a hitherto unknown genomic complexity in fungal viruses. *Virus Evol* 2021;7:veaa101.
8. Jia J, Fu Y, Jiang D, Mu F, Cheng J, et al. terannual dynamics, diversity and evolution of the virome in *Sclerotinia sclerotiorum* from a single crop field. *Virus Evol* 2021;7:veab032.
9. Kotta-Loizou I, Coutts RHA. Studies on the virome of the entomopathogenic fungus *Beauveria bassiana* reveal novel dsRNA elements and mild hypervirulence. *PLoS Pathog* 2017;13:e1006183.
10. Ruiz-Padilla A, Rodríguez-Romero J, Gómez-Cid I, Pacifico D, Ayllón MA. Novel mycoviruses discovered in the mycovirome of a necrotrophic fungus. *mBio* 2021;12:e03705-20:e03705-03720..
11. Sutela S, Forgia M, Vainio EJ, Chiapello M, Daghighi S, et al. The virome from a collection of endomycorrhizal fungi reveals new viral taxa with unprecedented genome organization. *Virus Evol* 2020;6:veaa076.
12. Hillman BI, Annisa A, Suzuki N. Viruses of plant-interacting fungi. *Adv Virus Res* 2018;100:99–116.
13. Vainio EJ, Pennanen T, Rajala T, Hantula J. Occurrence of similar mycoviruses in pathogenic, saprotrophic and mycorrhizal fungi inhabiting the same forest stand. *FEMS Microbiology Ecology* 2017;93:fix003.
14. Myers JM, Bonds AE, Clemons RA, Thapa NA, Simmons DR, et al. Survey of early-diverging lineages of fungi reveals abundant and diverse mycoviruses. *mBio* 2020;11:e02027-02020.
15. Gilbert KB, Holcomb EE, Allscheid RL, Carrington JC. Hiding in plain Insight: New virus genomes discovered via a systematic analysis of fungal public transcriptomes. *PLoS One* 2019;14:e0219207.
16. Zhang R, Hisano S, Tani A, Kondo H, Kanematsu S, et al. A capsidless ssRNA virus hosted by an unrelated dsRNA virus. *Nat Microbiol* 2016;1:15001.
17. Sato Y, Shamsi W, Jamal A, Bhatti MF, Kondo H, et al. Hadaka virus 1: a capsidless eleven-segmented positive-sense single-stranded rna virus from a phytopathogenic fuVirus 1: a Capsidless Eleven-Segmented Positive-Sense Single-Stranded RNA Virus from a Phytopathogenic Fungus, *Fusarium oxysporum*. *mBio* 2020;11:e00450-00420.
18. Kanhayuwa L, Kotta-Loizou I, Özkan S, Gunning AP, Coutts RHA. A novel mycovirus from *Aspergillus fumigatus* contains four unique dsRNAs as its genome and is infectious as dsRNA. *Proc Natl Acad Sci U S A* 2015;112:9100–9105.
19. Liu L, Xie J, Cheng J, Fu Y, Li G, et al. Fungal negative-stranded RNA virus that is related to bornaviruses and nyaviruses. *Proc Natl Acad Sci U S A* 2014;111:12205–12210.
20. Lin Y-H, Fujita M, Chiba S, Hyodo K, Andika IB, et al. Two novel fungal negative-strand RNA viruses related to mymonaviruses and phenoviruses in the shiitake mushroom (*Lentinula edodes*). *Virology* 2019;533:125–136.
21. Yu X, Li B, Fu Y, Jiang D, Ghabrial SA, et al. A geminivirus-related DNA mycovirus that confers hypovirulence to a plant pathogenic fungus. *Proc Natl Acad Sci U S A* 2010;107:8387–8392.
22. Li PF, Wang SC, Zhang LH, Qiu DW, Zhou XP, et al. A tripartite ssDNA mycovirus from a plant pathogenic fungus is infectious as cloned DNA and purified virions. *Sci Adv* 2020;6:14.
23. Feng C, Feng J, Wang Z, Pedersen C, Wang X, et al. Identification of the viral determinant of hypovirulence and host range in Sclerotiniaceae of a genomovirus reconstructed from the plant metagenome. *J Virol* 2021;95:e0026421.
24. Vainio EJ, Sutela S. Mixed infection by a partitivirus and a negative-sense RNA virus related to mymonaviruses in the polypore fungus *Bondarzewia berkeleyi*. *Virus Res* 2020;286:198079.
25. Osaki H, Sasaki A, Nomiya K, Tomioka K. Multiple virus infection in a single strain of *Fusarium poae* shown by deep sequencing. *Virus Genes* 2016;52:835–847.
26. Doherty M, Coutts RHA, Brasier CM, Buck KW. Sequence of RNA-dependent RNA polymerase genes provides evidence for three more distinct mitoviruses in *Ophiostoma novo-ulmi* isolate Ld. *Virus Genes* 2006;33:41–44.
27. Sasaki A, Nakamura H, Suzuki N, Kanematsu S. Characterization of a new megabirnavirus that confers hypovirulence with the aid of a co-infecting partitivirus to the host fungus, *Rosellinia necatrix*. *Virus Res* 2016;219:73–82.
28. Hillman BI, Suzuki N. Viruses of the chestnut blight fungus, *Cryphonectria parasitica*. *Adv Virus Res* 2004;63:423–472.
29. Kondo H, Kanematsu S, Suzuki N. Viruses of the white root rot fungus, *Rosellinia necatrix*. *Adv Virus Res* 2013;86:177–214.
30. Xie J, Jiang D. New insights into mycoviruses and exploration for the biological control of crop fungal diseases. *Annu Rev Phytopathol* 2014;52:45–68.
31. Cho WK, Lee KM, Yu J, Son M, Kim KH. sight into mycoviruses infecting *Fusarium* species. *Adv Virus Res* 2013;86:273–288.
32. Li P, Bhattacharjee P, Wang S, Zhang L, Ahmed I, et al. Mycoviruses in *Fusarium* species: An update. *Front Cell Infect Microbiol* 2019;9:257.
33. Jamal A, Sato Y, Shahi S, Shamsi W, Kondo H, et al. Novel victoriavirus from a Pakistani isolate of *Alternaria alternata* lacking a typical translational stop/restart sequence signature. *Viruses* 2019;11:577.
34. Shamsi W, Sato Y, Jamal A, Shahi S, Kondo H, et al. Molecular and biological characterization of a novel botybirnavirus identified from a Pakistani isolate of *Alternaria alternata*. *Virus Res* 2019;263:119–128.
35. Khan HA, Sato Y, Kondo H, Jamal A, Bhatti MF, et al. A second capsidless hadakavirus strain with 10 positive-sense single-stranded RNA genomic segments from *Fusarium nygamai*. *Arch Virol* 2021;166:2711–2722.
36. Sato Y, Jamal A, Kondo H, Suzuki N. Molecular characterization of a novel polymycovirus from *Penicillium janthinellum* with a focus on its genome-associated PASrp. *Front Microbiol* 2020;11:2523.
37. Bhatti MF, Jamal A, Bignell EM, Petrou MA, Coutts RHA. Incidence of dsRNA mycoviruses in a collection of *Aspergillus fumigatus* isolates. *Mycopathologia* 2012;174:323–326.
38. Eusebio-Cope A, Suzuki N. Mycoreovirus genome rearrangements associated with RNA silencing deficiency. *Nucleic Acids Res* 2015;43:3802–3813.
39. White TJ, Bruns T, Lee S, Taylor J. Amplification and direct sequencing of fungal ribosomal RNA genes for phylogenetics. In: Innis MA, Gelfand DH, Sninsky JJ and White TJ (eds). *PCR Protocols: A Guide to Methods and Applications*. New York, USA: Academic Press; 1990. pp. 315–322.
40. Appel DJ, Gordon TR. Relationships among pathogenic and nonpathogenic isolates of *Fusarium oxysporum* based on the partial sequence of the intergenic spacer region of the ribosomal DNA. *MPMI* 1996;9:125.
41. Marchler-Bauer A, Bo Y, Han L, He J, Lanczycki CJ, et al. CDD/SPARCLE: functional classification of proteins via subfamily domain architectures. *Nucleic Acids Res* 2017;45:D200–D203.
42. Katoh K, Toh H. Recent developments in the MAFFT multiple sequence alignment program. *Briefings in Bioinformatics* 2008;9:286–298.
43. Guindon S, Dufayard J-F, Lefort V, Anisimova M, Hordijk W, et al. New algorithms and methods to estimate maximum-likelihood phylogenies: assessing the performance of PhyML 3.0. *Syst Biol* 2010;59:307–321.
44. Nerva L, Varese GC, Falk BW, Turina M. Mycoviruses of an endophytic fungus can replicate in plant cells: evolutionary implications. *Sci Rep* 2017;7:1908.

45. Bartholomäus A, Wibberg D, Winkler A, Pühler A, Schlüter A, et al. Deep sequencing analysis reveals the mycoviral diversity of the virome of an avirulent isolate of *Rhizoctonia solani* AG-2-2 IV. *PLoS One* 2016;11:e0165965.
46. Koonin EV, Dolja VV, Krupovic M. Origins and evolution of viruses of eukaryotes: The ultimate modularity. *Virology* 2015;2–25.
47. Nibert ML, Ghabrial SA, Maiss E, Lesker T, Vainio EJ, et al. Taxonomic reorganization of family *Partitiviridae* and other recent progress in partitivirus research. *Virus Res* 2014;188:128–141.
48. Vainio EJ, Chiba S, Ghabrial SA, Maiss E, Roossinck M, et al. ICTV Virus Taxonomy Profile: *Partitiviridae*. *J Gen Virol* 2018;99:17–18.
49. Sasaki A, Miyanishi M, Ozaki K, Onoue M, Yoshida K. Molecular characterization of a partitivirus from the plant pathogenic ascomycete *Rosellinia necatrix*. *Arch Virol* 2005;150:1069–1083.
50. Yang Z, Geng H, Zheng Y, Yuan Y, Wang M, et al. Molecular characterization of a new gammapartitivirus isolated from the citrus-pathogenic fungus *Penicillium digitatum*. *Arch Virol* 2018;163:3185–3189.
51. Zhong J, Chen D, Lei XH, Zhu HJ, Zhu JZ, et al. Detection and characterization of a novel gammapartitivirus in the phytopathogenic fungus *Colletotrichum acutatum* strain HN2J001. *Virus Res* 2014;190:104–109.
52. Li S, Li Y, Hu C, Han C, Zhou T, et al. Full genome sequence of a new mitovirus from the phytopathogenic fungus *Rhizoctonia solani*. *Arch Virol* 2020;165:1719–1723.
53. Ayllón MA, Turina M, Xie J, Nerva L, Marzano S-YL, et al. ICTV Virus Taxonomy Profile: *Botourmiaviridae*. *J Gen Virol* 2020;101:454–455.
54. Nerva L, Ciuffo M, Vallino M, Margaria P, Varese GC, et al. Multiple approaches for the detection and characterization of viral and plasmid symbionts from a collection of marine fungi. *Virus Research* 2016;219:22–38.
55. Chu Y-M, Lim W-S, Yea S-J, Cho J-D, Lee Y-W, et al. Complexity of dsRNA mycovirus isolated from *Fusarium graminearum*. *Virus Genes* 2004;28:135–143.
56. Picarelli MASC, Forgia M, Rivas EB, Nerva L, Chiapello M, et al. Extreme diversity of mycoviruses present in isolates of *Rhizoctonia solani* AG2-2 LP from *Zoysia japonica* from Brazil. *Front Cell Infect Microbiol* 2019;9:244.
57. Chiba S, Kondo H, Tani A, Saisho D, Sakamoto W, et al. Widespread endogenization of genome sequences of non-retroviral RNA viruses into plant genomes. *PLoS Pathog* 2011;7:e1002146.
58. Liu H, Fu Y, Jiang D, Li G, Xie J, et al. Widespread horizontal gene transfer from double-stranded RNA viruses to eukaryotic nuclear genomes. *J Virol* 2010;84:11876–11887.
59. Aulia A, Tabara M, Telengech P, Fukuhara T, Suzuki N. Dicer monitoring in a model filamentous fungus host, *Cryphonectria parasitica*. *Current Research in Virological Science* 2020;1:100001.
60. Arjona-López JM, Telengech P, Suzuki N, López-Herrera CJ. Coinfection of *Rosellinia necatrix* by a partitivirus and a virga-like virus is associated with hypovirulence. *Eur J Plant Pathol* 2020;158:111–119.
61. Nerva L, Silvestri A, Ciuffo M, Palmano S, Varese GC, et al. Transmission of *Penicillium aurantiogriseum* partiti-like virus 1 to a new fungal host (*Cryphonectria parasitica*) confers higher resistance to salinity and reveals adaptive genomic changes. *Environ Microbiol* 2017;19:4480–4492.
62. Sasaki A, Kanematsu S, Onoue M, Oikawa Y, Nakamura H, et al. Artificial infection of *Rosellinia necatrix* with purified viral particles of a member of the genus *Mycovirus* reveals its uneven distribution in single colonies. *Phytopathology* 2007;97:278–286.
63. Salapeth L, Chiba S, Eusebio-Cope A, Kanematsu S, Suzuki N. Biological properties and expression strategy of *rosellinia necatrix* megabirnavirus 1 analysed in an experimental host, *Cryphonectria parasitica*. *J Gen Virol* 2014;95:740–750.
64. Chiba S, Lin YH, Kondo H, Kanematsu S, Suzuki N. A novel betapartitivirus RnPV6 from *Rosellinia necatrix* tolerates host RNA silencing but is interfered by its defective RNAs. *Virus Res* 2016;219:62–72.
65. Chiba S, Lin YH, Kondo H, Kanematsu S, Suzuki N. A novel victorivirus from a phytopathogenic fungus, *Rosellinia necatrix*, is infectious as particles and targeted by RNA silencing. *J Virol* 2013;87:6727–6738.
66. Shahi S, Chiba S, Kondo H, Suzuki N. *Cryphonectria nitschkei* chrysovirus 1 with unique molecular features and a very narrow host range. *Virology* 2021;554:55–65.
67. Kanematsu S, Sasaki A, Onoue M, Oikawa Y, Ito T. Extending the fungal host range of a partitivirus and a mycovirus from *Rosellinia necatrix* by inoculation of protoplasts with virus particles. *Phytopathology* 2010;100:922–930.
68. Hillman BI, Esteban R. Narnaviridae. In: King AMQ, Adams MJ, Carstens EB and Lefkowitz EJ (eds). *Virus Taxonomy: Classification and Nomenclature of Viruses: Ninth Report of the International Committee on Taxonomy of Viruses*. San Diego: Elsevier; 2011.
69. Walker PJ, Siddell SG, Lefkowitz EJ, Mushegian AR, Adriaenssens EM, et al. Changes to virus taxonomy and the Statutes ratified by the International Committee on Taxonomy of Viruses (2020). *Arch Virol* 2020;165:2737–2748.
70. Nibert ML, Debat HJ, Manny AR, Grigoriev IV, De Fine Licht HH. Mitovirus and mitochondrial coding sequences from basal fungus *Entomophthora muscae*. *Viruses* 2019;11:E351.
71. Liu JJ, Chan D, Xiang Y, Williams H, Li XR, et al. Characterization of five novel mitoviruses in the white pine blister rust fungus *Cronartium ribicola*. *PLoS One* 2016;11:e0154267.
72. Howitt RLJ, Beever RE, Pearson MN, Forster RLS. Genome characterization of a flexuous rod-shaped mycovirus, Botrytis virus X, reveals high amino acid identity to genes from plant “potex-like” viruses. *Arch Virol* 2006;151:563–579.
73. Hong YG, Dover SL, Cole TE, Brasier CM, Buck KW. Multiple mitochondrial viruses in an isolate of the Dutch elm disease fungus *Ophiostoma novo-ulmi*. *Virology* 1999;258:118–127.
74. Liu Y, Zhang L, Esmail A, Duan J, Bian X, et al. Four novel botourmiaviruses co-infecting an isolate of the rice blast fungus *Magnaporthe oryzae*. *Viruses* 2020;12:12.
75. Shahi S, Eusebio-Cope A, Kondo H, Hillman BI, Suzuki N. Investigation of host range of and host defense against a mitochondrially replicating mitovirus. *J Virol* 2019;93:e01503-01518.
76. Donaie L, Ayllón MA. Deep sequencing of mycovirus-derived small RNAs from *Botrytis* species. *Mol Plant Pathol* 2017;18:1127–1137.
77. Nerva L, Vigani G, Di Silvestre D, Ciuffo M, Forgia M, et al. Biological and molecular characterization of *Chenopodium quinoa* mitovirus 1 reveals a distinct small RNA response compared to those of cytoplasmic RNA viruses. *J Virol* 2019;93:e01998-01918.
78. Ohkita S, Lee Y, Nguyen Q, Ikeda K, Suzuki N, et al. Three ourmiaviruses and their associated RNAs in *Pyricularia oryzae*. *Virology* 2019;534:25–35.
79. Polashock JJ, Hillman BI. A small mitochondrial double-stranded (ds) RNA element associated with a hypovirulent strain of the chestnut blight fungus and ancestrally related to yeast cytoplasmic T and W dsRNAs. *Proc Natl Acad Sci U S A* 1994;91:8680–8684.
80. Crivelli G, Ciuffo M, Genre A, Masenga V, Turina M. Reverse genetic analysis of Ourmiaviruses reveals the nucleolar localization of the coat protein in *Nicotiana benthamiana* and unusual requirements for virion formation. *J Virol* 2011;85:5091–5104.
81. Wang Q, Mu F, Xie J, Cheng J, Fu Y, et al. A single ssRNA segment encoding RdRp is sufficient for replication, infection, and transmission of ourmia-like virus in fungi. *Front Microbiol* 2020;11.